European Review for Medical and Pharmacological Sciences 2022; 26: 8265-8275

Molecular mechanism of Tongmai Yangxin Pill intervention in elderly patients with coronary heart disease

Z.-W. XIAO[1], Y. LIU[2], Z.-Y. LI[3], S. LI[4], L.-H. QIN[2,3]

[1]Department of Food and Drug Engineering, School of Pharmacy, [2]Key Laboratory of Hunan Province for Prevention and Treatment of Integrated Traditional Chinese and Western Medicine on Cardiocerebral Diseases, [3]School of Nursing, [4]School of Informatics, Hunan University of Chinese Medicine, Hunan, Changsh, P.R. China

Zuowei Xiao and Yang Liu contributed equally to this study and are considered co-first authors

Abstract. – OBJECTIVE: The Tongmai Yangxin Pill (TMYX) is considered an effective treatment for coronary heart disease (CHD). However, its mechanism is unclear. This study aimed at exploring the molecular mechanisms and key genes of the TMYX in the treatment of CHD.

MATERIALS AND METHODS: Differentially expressed genes (DEGs) in the GSE142008 dataset were screened with the R software, and Gene Ontology (GO) and Kyoto Encyclopedia of Genes and Genomes (KEGG) enrichment analyses were performed. Then, protein-protein interactions were analyzed using the Search Tool for the Retrieval of Interacting Genes database. The correlation analysis between key genes was conducted, and gene expression was verified.

RESULTS: A total of 1,614 DEGs were identified, including 1,591 upregulated and 23 downregulated genes. GO enrichment analysis revealed that 240 biological processes, 44 cellular components, and 23 molecular functions were significantly enriched for DEGs in elderly patients with CHD. Similarly, 36 KEGG terms were significantly enriched for DEGs. Ten key genes were screened, and after verification and analysis, seven key genes (*RSL24D1, NMD3, DCAF13, WDR36, SDAD1, KRR1*, and *RPF1*) were identified as significantly overexpressed.

CONCLUSIONS: We identified seven key genes as candidate biomarkers for TMYX in the treatment of elderly patients with CHD; these results can serve as a theoretical basis for targeted therapy.

Key Words:
Tongmai Yangxin Pill, Coronary Heart Disease, Elderly, Differential mRNA Expression.

Abbreviations

TMYX, Tongmai Yangxin Pill; CHD, coronary heart disease; GEO, Gene Expression Omnibus; DEGs, differentially expressed genes; GO, Gene Ontology; KEGG, Kyoto Encyclopedia of Genes and Genomes; PPI, protein-protein interaction; BP, biological process; CC, cellular component; MF, molecular function.

Introduction

Coronary heart disease (CHD) is caused by coronary artery atherosclerosis and stenosis or obstruction, resulting in myocardial ischemia, hypoxia, or necrosis[1]. CHD has high incidence and mortality rates. It is estimated that more than 23.6 million people will die from cardiovascular diseases by 2030, with CHD being the leading cause of death[2]. The incidence and mortality of patients with CHD continue to rise in China due to the aging population and increasing urbanization[3], causing an emotional burden to families and a financial load to society. Therefore, it is essential to study the mechanisms underlying CHD treatment in the elderly to better control CHD, reduce the associated burden on families, and curtail the socioeconomic pressure on society.

Significant progress has been made in treating CHD, particularly for drugs and surgical treatments[4]. Conventional treatment drugs include beta-blockers, calcium channel blockers, antiplatelet drugs, and anticoagulants[5]; however, associated side effects include headache, gastrointestinal reaction, bleeding, hypotension, and rash, among others[5,6]. Traditional Chinese medicine has been used to treat CHD, with a significant curative effect and limited side effects; thus, it has attracted extensive attention in recent years[6]. The Tongmai Yangxin Pill

Corresponding Author: Lihua Qin, MD; e-mail: 479157643@qq.com

(TMYX), a patented drug, has been widely used to treat CHD in China. Although anti-inflammatory properties seem to underly the mode of action of TMYX in CHD treatment[7], the detailed mechanism remains unclear. This study aimed at exploring the molecular mechanism and hub genes of the TMYX in treating elderly patients with CHD using a bioinformatics approach to provide new concepts to treat CHD and further develop traditional Chinese medicines.

Materials and Methods

Dataset Searching and Preprocessing

The GSE142008 dataset was downloaded from the Gene Expression Omnibus (GEO) website using the GPL570 (HG-U133_Plus_ 2.) Affymetrix Human Genome U133 Plus 2.0 Array platform. The GEO datasets included eight patients with CHD before TMYX treatment and eight patients with CHD after TMYX treatment for 8 weeks. The GSE142008 dataset consisted of 16 peripheral blood mononuclear cell samples from patients with CHD, aged 49-66 years. According to the study design, peripheral blood mononuclear cells of six patients (age ≥ 60 years) before treatment were considered as the control group (group 1), and peripheral blood mononuclear cells of six patients (age ≥ 60 years) after treatment with TMYX were considered as the experimental group (group 2).

The R software (version 3.6.3, The R Foundation for Statistical Computing, Vienna, Austria) was used for statistical analysis and visualization of data processing; the UMAP package (version 0.2.7.0) was used for Uniform Manifold Approximation and Projection (UMAP) analysis; the ggplot2 package (version 3.3.3) was used to visualize the data normalization box plots, principal component analysis (PCA) plots, and UMAP plots.

Genomic Analysis of Differentially Expressed Genes (DEGs)

Probes with no gene annotation or multiple matched gene symbols were removed. DEGs of the GSE142008 dataset between groups 1 and 2 were screened by the "limma" R package, with a cut-off criterion of $|\log_2 \text{fold change (FC)}| \geq 1$ and an adjusted *p*-value (Benjamini-Hochberg method) < 0.05. The R software (version 3.6.3) was used for statistical analysis and visualization; the "complexheatmap" package (version 2.2.0) was used to visualize the heat map for the distribution and expression of the identified DEGs, and the "ggplot2" (version 3.6.3) package was used to visualize the volcano plot[8].

Gene Ontology (GO) and Kyoto Encyclopedia of Genes and Genomes (KEGG) Combined logFC enrichment Analysis Pathway

Based on GO and KEGG enrichment analyses using the R software (version 3.6.3), we calculated the Z-score corresponding to each entry using the logFC of the provided molecules, and preliminarily determined whether the corresponding entry was a positive (Z-score > 0) or negative (Z-score < 0) regulation. The "org.Hs.eg.db" package (version 3.10.0) was used for ID conversion; the "clusterprofiler" package (version 3.14.3) was used for enrichment analysis. The "goplot" package (version 1.0.2) was used to calculate the Z-score. The "goplot" and "ggplot2" packages (version 3.3.3) were used to produce the column chart and circle chart, respectively[9,10]. An adjusted *p*-value of < 0.05 and a q-value of < 0.2 indicated statistically significant enrichment during the GO and KEGG analyses.

Analysis of Protein-Protein Interaction Networks and Key Genes

Using the Search Tool for the Retrieval of Interacting Genes Database (STRING; http://string-db.org)[11], protein-protein interaction (PPI) analyses were performed for different genes, with an interaction score threshold of 0.40. Next, the results were imported into the Molecular Complex Detection (MCODE) and cytoHubba plug-in of the Cytoscape (version 3.8.2) software to screen the key genes.

Statistical Analysis

The "ggplot2" (version 3.3.3) and "circlize" (version 0.4.12) packages of R were used for correlation analyses and to visualize the correlation heat map and chord map (correlation circle map). In a chord map, if the correlation coefficient between a molecule and other molecules is large, the total length of the color block of this molecule will be relatively long. R (version 3.6.3) was used for all statistical analyses of expression profiles of key genes, and the "ggplot2" package was used for visualization. A *p*-value of < 0.05 was considered statistically significant (all *p*-values presented are two-sided).

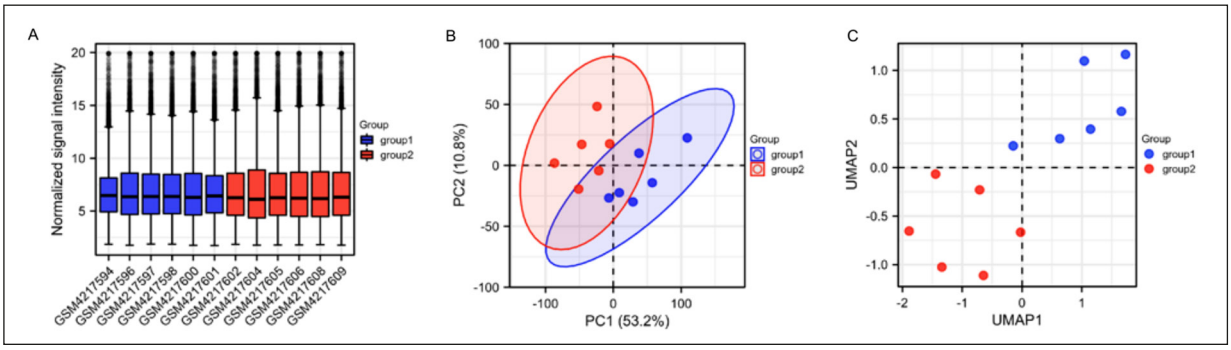

Figure 1. Normalization and clustering of samples. **A,** Box chart; **B,** PCA diagram; **C,** UMAP diagram. The blue bars represent the normalized data of the group 1, and the red bars represent the normalized data of the group 2. The group 1 was the control group; the group 2 was the experimental group.

Results

Data Preprocessing

The results of the box chart showed that the median of all samples essentially laid on a horizontal line, indicating that the normalization degree between samples was good and that samples could be compared in parallel (Figure 1A). The PCA and UMAP diagram determined that the groups of samples were separated (Figures 1B and 1C).

Identification of DEGs

Overall, 1,614 specific DEGs, including 1,591 highly expressed genes and 23 downregulated genes, were identified the elderly patients with CHD before and after TMYX treatment (Table I). The volcano plot in Figure 2A shows the expression of DEGs. The top ten upregulated and downregulated DEGs are listed in Table I, and the corresponding heat map is shown in Figure 2B.

GO and KEGG Enrichment Analyses

GO enrichment analysis included the following: biological processes (BP), cellular components (CC), and molecular functions (MF). A total of 240 BP, 44 CC, and 23 MF were significantly enriched for DEGs in elderly patients with CHD (p-value < 0.05). Furthermore, we found that

Table I. Top 10 upregulated and downregulated DEGs of patient with CHD after treatment compared to patient with CHD before treatment.

Gene ID	Gene symbol	Adj. *p*-value	logFC	Up/Down
204774_at	EVI2A	0.004	2.639	Up
201921_at	GNG10	0.002	2.548	Up
223809_at	RGS18	0.001	2.526	Up
201238_s_at	CAPZA2	0.001	2.421	Up
219540_at	ZNF267	0.001	2.399	Up
224866_at	FAR1	0.001	2.382	Up
222850_s_at	DNAJB14	0.001	2.334	Up
200032_s_at	RPL9	0.031	2.240	Up
202769_at	CCNG2	0.001	2.197	Up
224786_at	SCOC	0.003	2.169	Up
1569105_at	SETD5	0.017	-1.560	Down
215684_s_at	ASCC2	0.026	-1.301	Down
200001_at	CAPNS1	0.003	-1.286	Down
396_f_at	EPOR	0.019	-1.218	Down
203154_s_at	PAK4	0.006	-1.210	Down
1556900_at	APCDD1L-AS1	0.013	-1.158	Down
201052_s_at	PSMF1	0.036	-1.115	Down
213175_s_at	SNRPB	0.009	-1.096	Down
217040_x_at	SOX15	0.020	-1.091	Down
211531_x_at	PRB1	0.022	-1.068	Down

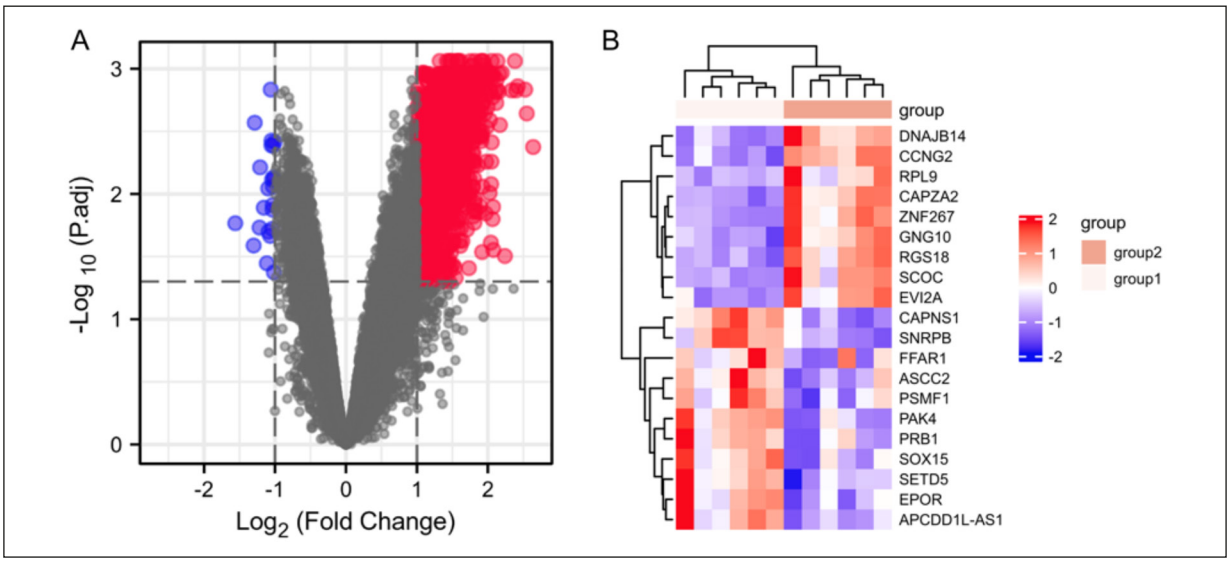

Figure 2. Volcano plot and of Heat map DEGs. **A,** Volcano plot of DEGs. Genes without any significant difference are marked with gray dots, upregulated genes are marked with red dots, and downregulated genes with blue dots. **B,** Heat map of the significantly altered genes. The color size corresponding to the converted value of zscore. Red represents high and blue represents low.

36 KEGG terms were significantly enriched for DEGs. Table II summarizes the top five results of the BP, CC, MF, and ten KEGG analyses. The BP, CC, and MF enrichment results, in addition to those of the subsequent KEGG pathway, are displayed in Figure 3A-D. The "up" and "down" represent the number of positive and negative logFC of the corresponding entry molecule, respectively. The greater was the absolute value of the Z-score, the greater was the difference in the number of upregulated and downregulated molecules, indicating that the degree of regulation may be higher.

Analysis of PPI Network and Key Gene Selection

The STRING database (version 11.0, https://www.string-db.org/) was used to assess the PPIs among the products of the DEGs[11]. The STRING database with a confidence score > 0.4 was used, and the PPI network was visualized with the Cytoscape 3.8.2 software (Figure 4). The MCODE and cytoHubba plug-ins of Cytoscape were used to identify hub genes. The results of the MCODE indicated ten clusters. Cluster 1, with the highest score of 14.286, 100 nodes, and 100 edges, was selected. According to the MCODE score ranking, 15 DEGs played a key role in elderly patients with CHD, including KRR1, the small subunit processome component homolog (*KRR1*), DDB1 and CUL4 associated factor 13 (*DCAF13*), WD repeat domain 36 (*WDR36*), transcription factor B2, mitochondrial (*TFB2M*), DEAH-box helicase 15 (*DHX15*), NMD3 ribosome export adaptor (*NMD3*), SDA1 domain containing 1 (*SDAD1*), nucleolar protein interacting with the fork-head associated (FHA) domain of MKI67 (*NIFK*), ribosome production factor 1 homolog (*RPF1*), ESF1 nucleolar pre-rRNA processing protein homolog (*ESF1*), UTP23, a small subunit processome component (*UTP23*), ribosomal L24 domain containing 1 (*RSL24D1*), GTP binding protein 4 (*GTPBP4*), CCAAT/enhancer binding protein zeta (*CEBPZ*), and Ski2-like RNA helicase 2 (*SKIV2L2*; Figure 5A). According to the descending scores determined by the maximum cross-correlation method of cytoHubba, the key genes ordered by decreasing expression were *RSL24D1*, *NMD3*, *GTPBP4*, *DCAF13*, *WDR36*, *SDAD1*, *KRR1*, *NIFK*, *CEBPZ*, and *RPF1* (Figure 5B).

Correlation Analysis Between Key Genes

The results showed strong positive correlations between *RSL24D1* and *NMD3*; *NMD3* and *GTPBP4*, *DCAF13*, *WDR36*, *SDAD1*, *KRR1*, and *NIFK*; *GTPBP4* and *DCAF13*, *WDR36*, *SDAD1*, *KRR1*, and *NIFK*; *DCAF13* and *WDR36*, *SDAD1*,

Table II. GO/KEGG analysis results of the identified gender-specific genes.

Ontology	ID	Description	GeneRatio	BgRatio	*p*-value	*p* adjust	q-value
BP	GO:0010498	Proteasomal protein catabolic process	85/1,397	477/18,670	3.93e-14	1.17e-10	1.04e-10
BP	GO:0043161	Proteasome-mediated ubiquitin-dependent protein catabolic process	78/1,397	419/18,670	4.19e-14	1.17e-10	1.04e-10
BP	GO:0002221	Pattern recognition receptor signaling pathway	39/1,397	197/18,670	1.74e-08	2.94e-05	2.59e-05
BP	GO:0002758	Innate immune response-activating signal transduction	51/1,397	298/18,670	2.10e-08	2.94e-05	2.59e-05
BP	GO:0002224	Toll-like receptor signaling pathway	32/1,397	146/18,670	2.69e-08	3.01e-05	2.66e-05
CC	GO:0016607	Nuclear speck	67/1,458	397/19,717	1.50e-10	9.83e-08	8.11e-08
CC	GO:0016605	PML body	24/1,458	99/19,717	1.61e-07	5.29e-05	4.37e-05
CC	GO:0031965	Nuclear membrane	47/1,458	296/19,717	5.23e-07	1.14e-04	9.43e-05
CC	GO:0000151	Ubiquitin ligase complex	45/1,458	282/19,717	7.88e-07	1.26e-04	1.04e-04
CC	GO:0005635	Nuclear envelope	64/1,458	464/19,717	9.57e-07	1.26e-04	1.04e-04
MF	GO:0019003	GDP binding	21/1,403	74/17,697	1.67e-07	1.60e-04	1.45e-04
MF	GO:0019787	Ubiquitin-like protein transferase activity	62/1,403	407/17,697	4.57e-07	2.18e-04	1.98e-04
MF	GO:0004842	Ubiquitin-protein transferase activity	58/1,403	382/17,697	1.19e-06	3.63e-04	3.30e-04
MF	GO:0061630	Ubiquitin protein ligase activity	39/1,403	221/17,697	1.76e-06	3.63e-04	3.30e-04
MF	GO:0061659	Ubiquitin-like protein ligase activity	40/1,403	230/17,697	1.90e-06	3.63e-04	3.30e-04
KEGG	hsa04140	Autophagy-animal	28/608	137/8,076	8.59e-07	2.58e-04	1.93e-04
KEGG	hsa05161	Hepatitis B	29/608	162/8,076	9.01e-06	0.001	0.001
KEGG	hsa05163	Human cytomegalovirus infection	35/608	225/8,076	2.72e-05	0.003	0.002
KEGG	hsa05220	Chronic myeloid leukemia	17/608	76/8,076	3.67e-05	0.003	0.002
KEGG	hsa05132	Salmonella infection	37/608	249/8,076	4.49e-05	0.003	0.002
KEGG	hsa05215	Prostate cancer	19/608	97/8,076	9.11205E-05	0.004	0.003
KEGG	hsa04218	Cellular senescence	26/608	156/8,076	9.18808E-05	0.004	0.003
KEGG	hsa04068	FoxO signaling pathway	23/608	131/8,076	0.0001	0.004	0.003
KEGG	hsa04115	p53 signaling pathway	15/608	73/8,076	0.0002	0.009	0.006
KEGG	hsa04120	Ubiquitin mediated proteolysis	23/608	140/8,076	0.0002	0.009	0.006

KRR1, and *NIFK*; *WDR36* and *SDAD1*, *KRR1*, and *NIFK*; *SDAD1* and *KRR1* and *NIFK*; and *KRR1* and *NIFK* ($p < 0.05$; Figure 6A and Figure 5B).

Verification of Key Gene Expression Levels

The samples did not meet the normality test ($p < 0.05$); thus, a Mann-Whitney U test (Wilcoxon rank-sum test) was selected for analysis. The results showed that the expression of *RSL24D1*, *NMD3*, *DCAF13*, *WDR36*, *SDAD1*, *KRR1*, and *NIFK* increased significantly after TMYX treatment ($p < 0.05$) compared with that before treatment. The median differences between the two groups were 2.142 (0.794-2.493), 1.496 (0.639-2.007), 1.078 (0.321-2.306), 0.931 (0.422-1.914), 0.942 (0.362-1.889), 0.941 (0.488-1.387), and 0.809 (0.392-1.366), respectively. After TMYX treatment, the changes in the expression of *GTPBP4*, *CEBPZ*, and *RPF1* were not statistically significant ($p > 0.05$; Figure 7).

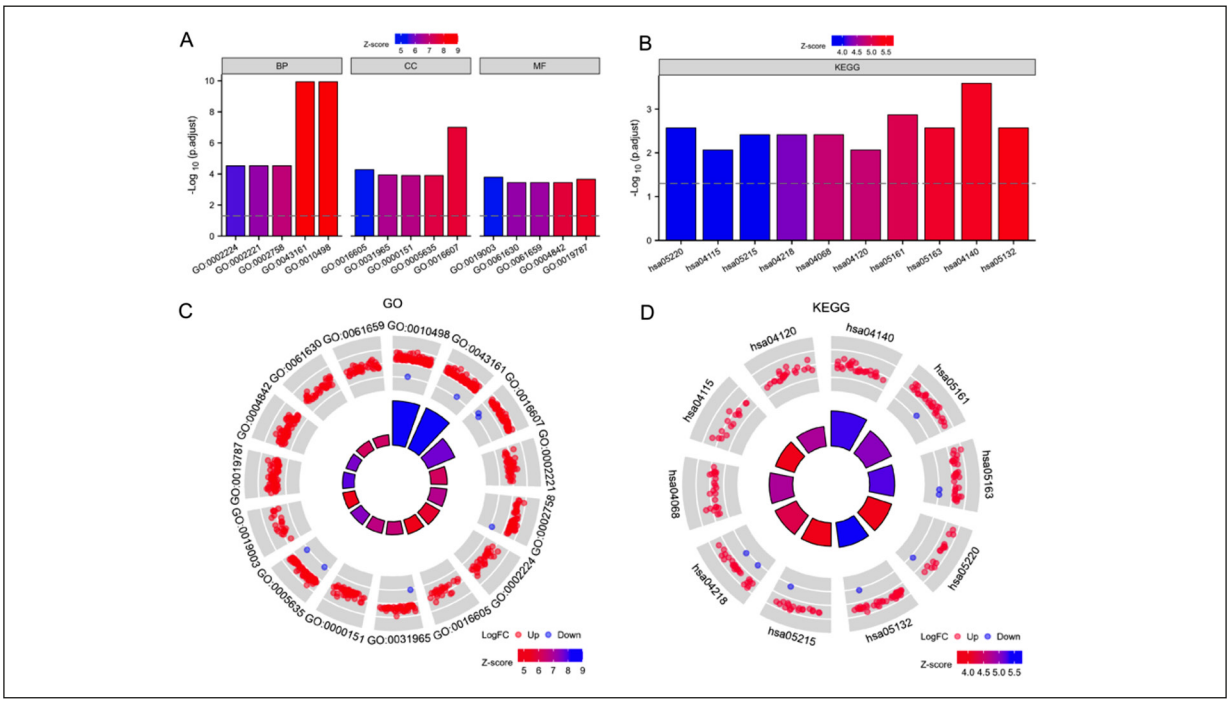

Figure 3. GO/KEGG joint logFC diagram analysis of DEGs. **A,** Column chart of GO; **B,** Column chart of KEGG; **C,** Circle chart of GO; **D,** Circle chart of KEGG. The up and down represent respectively the number of the positive and negative logFC of the corresponding entry molecule. The greater the absolute value of zscore, the greater the difference in the number of high expression molecules and low expression molecules, indicating that the degree of regulation may be higher.

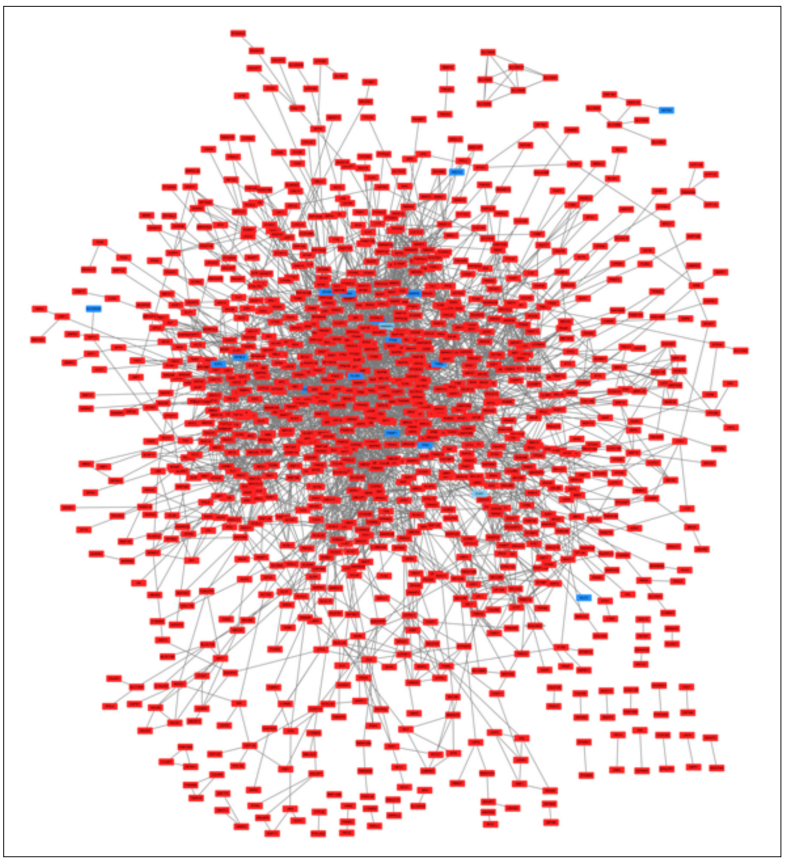

Figure 4. PPI network of DEGs. Red, upregulated genes, and blue, downregulated genes. PPI, protein-protein interaction; DEG, differentially expressed gene.

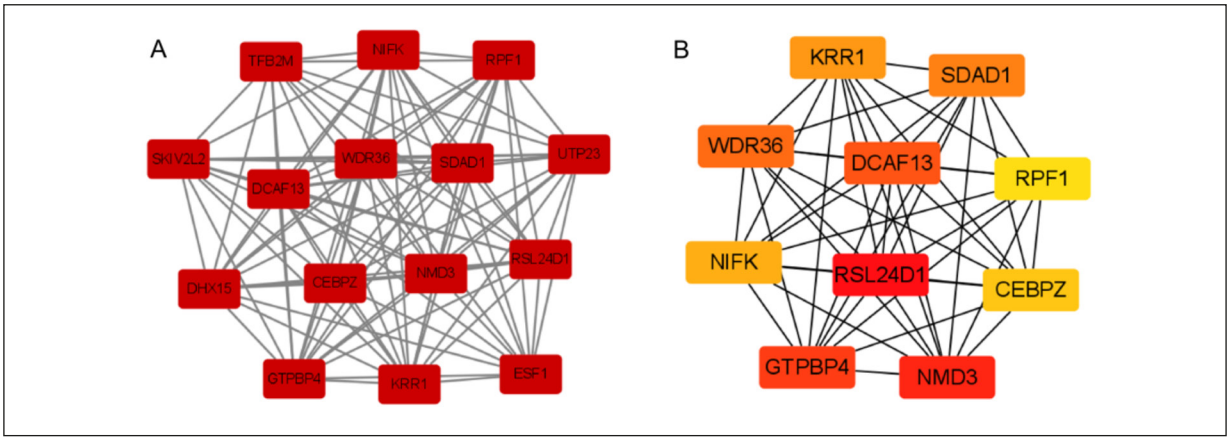

Figure 5. Key genes of DEGs. **A,** MCODE; **B,** cytoHubba. Nodes represent genes and lines represent interactions. RSL24D1 was marked in deep red as this is the gene with the highest degree in cytoHubba.

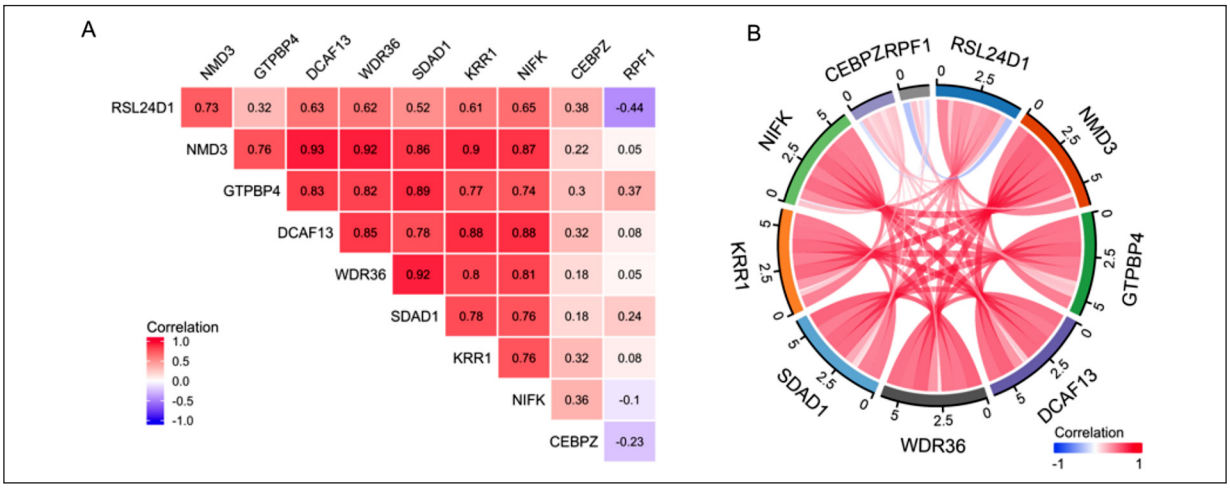

Figure 6. Correlation analysis of key genes. **A,** Correlation heat map. **B,** Chord map. The thickness of the band and the depth of the color represent the correlation. The greater the correlation (absolute value), the wider the band. Higher the intensity of blue color in the strip, the greater the negative correlation; and higher the intensity of red color, the greater the positive correlation.

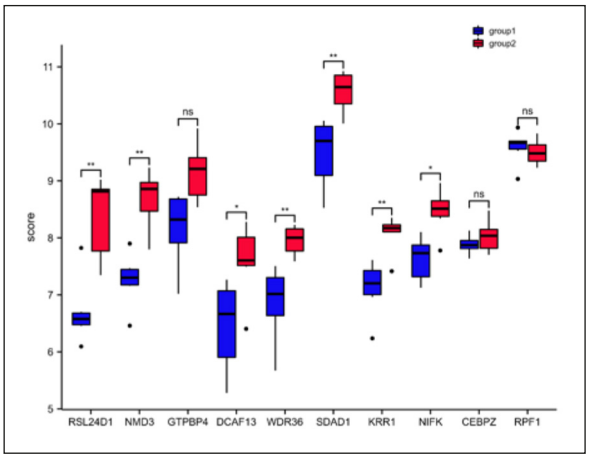

Figure 7. Expression analysis of key genes. Blue represents group 1 (the control group), and red represents group 2 (the experimental group). *$p < 0.05$; ** $p < 0.01$.

Discussion

CHD belongs to the categories of "heartache" and "chest arthralgia" in traditional Chinese medicine. Traditional Chinese medicine offers remarkable curative effects in treating CHD, with a long history and broad application prospects. The TMYX is a modern, patented Chinese medicine consisting of two classic traditional prescriptions: the Zhi Gancao Tang and Shengmai Yin. The TMYX comprises 11 traditional Chinese medicines, including licorice, *Rehmannia glutinosa*, Dangshen, prepared *Polygonum multiflorum*, *Ophiopogon japonicus*, *Schisandra chinensis*, donkey hide gelatin, vinegar tortoise shell, Caulis Spatholobi, cinnamon twig, and jujube. The TMYX exerts the effects of "supplementing Qi" and "nourishing Yin," dredging pulse, and relieving pain[12]. Since its listing, extensive clinical research has been conducted on the effects of TMYX in treating CHD and angina pectoris. Using the best available evidence combined with human expertise, more than 30 clinical and methodological experts in China have adopted the consensus development method developed by international clinical medical experts, indicating that TMYX can be used for the "Qi Yin deficiency syndrome" that characterizes CHD, angina pectoris, and arrhythmia[12]. Scholars[13] have demonstrated that TMYX plays a significant role in treating CHD by inhibiting inflammatory factors, protecting cardiomyocytes and vascular endothelium, and regulating hormone levels, among others.

In the current study, 1,614 DEGs were identified in peripheral blood mononuclear cells of elderly patients with CHD before and after treatment with TMYX, including 1,591 upregulated and 23 downregulated genes. The GO and KEGG enrichment analyses showed that a total of 240 BP, 44 CC, 23 MF, and 36 KEGG terms were significantly enriched for DEGs in elderly patients with CHD. A PPI network was constructed, and ten hub genes were identified. After verification, we determined that the gene expression of *RSL24D1*, *NMD3*, *DCAF13*, *WDR36*, *SDAD1*, *KRR1*, and *NIFK* was significantly increased after TMYX treatment compared with that before treatment.

RSL24D1 encodes ribosome biogenesis protein RLP24, which is functional in the biogenesis of the 60S ribosomal subunit. *RSL24D1* is related to familial hypercholesterolemia[14] and was reportedly significantly upregulated in patients with hypertension[15]. Familial hypercholesterolemia is a disorder with increased levels of low-density lipoprotein cholesterol, increasing the risk of atherosclerotic diseases, particularly CHD[16].

NMD3 is a highly conserved adaptor protein that is necessary for the nuclear export of the nascent 60S subunit in eukaryotes[17]. *LSG1* knockdown inhibits *NMD3* release from the ribosomal 60S subunit, and cellular senescence is strongly induced by inhibition of 60S maturation[18]. This finding suggests that *NMD3* is related to cellular senescence. Scholars[19] have proven that aging induces endothelial cell senescence, contributing to the development and progression of cardiovascular diseases.

DCAF13 belongs to the DDB1- and CUL4-related factor family and is the substrate receptor of CUL4-DDB1 E3 ligase[20]. Ubiquitination is closely related to cardiovascular disease. In particular, E3 ligases may play important roles in the progression of atherosclerosis[21], and E3 ubiquitin ligase can affect the regulation of large-conductance calcium-activated potassium channels in diabetic coronary artery disease[22]. In addition, the Caulis Spatholobi in TMYX is related to the ubiquitin protein hydrolysis pathway[23].

WDR36 is a protein-coding gene belonging to the WD repeat protein family. *WDR36* mRNA has been observed in the human heart and skeletal muscle. It participates in cell cycle processes, signal transduction, apoptosis, and gene regulation[24-27]. Although the exact function remains controversial, the deletion of *WDR36* mRNA in cultured cells leads to apoptosis, reduced 21S rRNA transcription, and delayed maturation of 18S rRNA[26,27]. *WDR36* gene knockout in zebrafish has demonstrated the importance of the gene in ribosomal biogenesis during nucleolar processing of 18srRNA[25]. Moreover, *WDR36* is important in the p53 stress response pathway, wherein *WDR36* knockout leads to the interruption of nucleolar function[27]. These considerations highlight the importance of *WDR36* in cell survival and function.

SDAD1, belonging to the SDAD family, was confirmed to be a direct target gene of miR378. It promotes the proliferation, migration, and invasion of colon cancer cells[28]. In addition, Ang II reportedly upregulated *SNHG7* and *SDAD1* in a cardiac hypertrophy model in neonatal rat cardiomyocytes; however, the effect of Ang II on cardiac hypertrophy was attenuated by silencing *SNHG7* and *SDADI*[29]. Another study[30] showed that circulating miRNA-378 was significantly

downregulated in the plasma of patients with CHD, and miRNA-738 expression was related to the severity of coronary artery lesions.

KRR1, a factor involved in ribosome assembly, is critical for cell viability. Previous scholars[30] suggest that *KRR1* is highly expressed in proliferating cells, whereas *KRR1* expression is almost completely halted when cells enter the quiescent phase. The maturation of ribosomes can induce apoptosis and inhibit the proliferation of vascular smooth muscle cells and macrophages, playing an anti-atherosclerotic role that is related to CHD[31].

NIFK encodes an RNA-binding protein, which is a nucleolar protein interacting with the FHA domain of the proliferation marker protein Ki-67[32,33]. Nucleolar proteins interacting with the FHA domain of MKI67 are necessary for cell cycle processes, participation in ribosomal biogenesis through its RNA recognition motif, and in G1 progression by interacting with rRNA processing[33].

The silencing of *NIFK* inhibited cell proliferation through a reversible p53-dependent G1 arrest[33]. p53 participates in regulating CVDs by regulating metabolism and programmed cell death to determine the fate of cardiomyocytes and control cell cycle arrest and angiogenesis in non-myocytes[34]. These studies indicate that *NIFK* is related to atherosclerosis and participates in the development of cardiovascular disease.

It is important to note that this study is limited because the function of these hub genes was not further confirmed experimentally. We plan to validate these results in future studies using peripheral blood mononuclear cells of patients with CHD, along with cellular and animal experiments.

Conclusions

We used GSE142008 datasets to identify DEGs related to the effects of TMYX in the treatment of CHD. We then screened the top ten signature genes in elderly patients with CHD. Among them, we validated seven key genes (*RSL24D1*, *NMD3*, *DCAF13*, *WDR36*, *SDAD1*, *KRR1*, and *RPF1*) as markers for predicting CHD and as potential indicators of the effectiveness of TMYX in the treatment of CDH in elderly patients. We hope these target genes might offer a new perspective for developing therapeutic and prognostic tools for CHD.

Conflict of Interest

The Authors declare that they have no conflict of interests.

Acknowledgements

The authors thank all individuals who participated in this study and donated samples.

Authors' Contribution

LHQ contributed to the study concept, design, and critical revision of the manuscript for important intellectual content. ZWX and YL performed data analysis and drafted the manuscript. SL and ZYL wrote the manuscript. All authors contributed to the revision of the manuscript. All authors read and approved the final manuscript.

Funding

This work was supported by the National Natural Science Foundation of China (No. 81904180) and the Hunan Provincial Department of Education Project (No. 20B429).

Availability of Data and Materials

The GSE142008 data used in our study are available via GEO (https://www.ncbi. nlm.nih.gov/). All data generated or analyzed during this study are included in this published article.

Ethics Approval

GEO is a public database. Our study is based on open-source data; hence, there are no ethical issues to declare.

Informed Consent

The patients involved in the database provided written consent.

References

1) Wu Y, Wang L, Zhan Y, Zhang Z, Chen D, Xiang Y, Xie C. The expression of SAH, IL-1β, Hcy, TNF-α and BDNF in coronary heart disease and its relationship with the severity of coronary stenosis. BMC Cardiovasc Disord 2022; 22: 101.
2) Writing Group Members, Mozaffarian D, Benjamin EJ, Go AS, Arnett DK, Blaha MJ, Cushman M, Das SR, de Ferranti S, Després JP, Fullerton HJ, Howard VJ, Huffman MD, Isasi CR, Jiménez MC, Judd SE, Kissela BM, Lichtman JH, Lisabeth LD, Liu S, Mackey RH, Magid DJ, McGuire DK, Mohler ER 3rd, Moy CS, Muntner P, Mussolino ME, Nasir K, Neumar RW, Nichol G, Palaniappan L, Pandey DK, Reeves MJ, Rodriguez CJ, Rosamond W, Sorlie PD, Stein J, Towfighi A,

Turan TN, Virani SS, Woo D, Yeh RW, Turner MB; American Heart Association Statistics Committee; Stroke Statistics Subcommittee. Heart Disease and Stroke Statistics-2016 Update: A Report from the American Heart Association. Circulation 2016; 133: e38-e360.

3) Hu SS, Gao RL, Liu LS, Zhu ML, Wang W, Wang YJ, Wu ZHJ, Li HJ, Gu DF, Y YJ, Zhang ZH, Chen WW, on behalf of the Writing Committee of the Report on Cardiovascular Diseases in China. Summary of the 2018 Report on Cardiovascular Diseases in China. Chinese Circulation Journal 2019; 34: 209-220.
4) Kandaswamy E, Zuo L. Recent advances in treatment of coronary artery disease: Role of science and technology. Int J Mol Sci 2018; 19: 424.
5) Guo XF, Chen JJ, Chen X. Research Progress of treatment of coronary heart disease in elderly patients. Medical Recapitulate 2021; 27: 2189-2193.
6) Zhang J, Meng H, Zhang Y, Zhang X, Shao M, Li C, Tu P. The Therapeutical effect of Chinese medicine for the treatment of atherosclerotic coronary heart disease. Curr Pharm Des 2017; 23: 5086-5096.
7) Fan Y, Liu J, Miao J, Zhang X, Yan Y, Bai L, Chang J, Wang Y, Wang L, Bian Y, Zhou H. Anti-inflammatory activity of the Tongmai Yangxin pill in the treatment of coronary heart disease is associated with estrogen receptor and NF-κB signaling pathway. J Ethnopharmacol 2021; 276: 114106.
8) Gu Z, Eils R, Schlesner M. Complex heatmaps reveal patterns and correlations in multidimensional genomic data. Bioinformatics 2016; 32: 2847-2849.
9) Yu G, Wang LG, Han Y, He QY. clusterProfiler: an R package for comparing biological themes among gene clusters. OMICS 2012; 16: 28-287.
10) Wencke W, Fátima SC, Mercedes R. GOplot: an R package for visually combining expression data with functional analysis. Bioinformatics 2015; 31: 2912-2914.
11) Szklarczyk D, Gable AL, Lyon D, Junge A, Wyder S, Huerta-Cepas J, Simonovic M, Doncheva NT, Morris JH, Bork P, Jensen LJ, Mering CV. STRING v11: protein-protein association networks with increased coverage, supporting functional discovery in genome-wide experimental datasets. Nucleic Acids Res 2019; 47: D607-D613.
12) Wang X, An DQ. Expert consensus on clinical application of TongmaiYangxin Pill in treatment of angina pectoris (Qi-Yin deficiency syndrome). Chinese Archives of Traditional Chinese Medicine 2021; 39: 253-258.
13) Liu ZHC, Wang ZH, Tang Q, Wang BH. Research Progress on mechanism and clinical application of Tongmai Yangxin pill in the treatment of coronary heart disease. JETCM 2018; 27: 1304-1306.
14) Li G, Wu XJ, Kong XQ, Wang L, Jin X. Cytochrome c oxidase subunit VIIb as a potential target in familial hypercholesterolemia by bioinformatical analysis. Eur Rev Med Pharmacol Sci 2015; 19: 4139-4145.
15) Peng W, Cao H, Liu K, Guo C, Sun Y, Qi H, Liu Z, Xie Y, Liu X, Li B, Zhang L. Identification of lncRNA-NR_104160 as a biomarker and construction of a lncRNA-related ceRNA network for essential hypertension. Am J Transl Res 2020; 12: 6060-6075.
16) Nordestgaard BG, Chapman MJ, Humphries SE, Ginsberg HN, Masana L, Descamps OS, Wiklund O, Hegele RA, Raal FJ, Defesche JC, Wiegman A, Santos RD, Watts GF, Parhofer KG, Hovingh GK, Kovanen PT, Boileau C, Averna M, Borén J, Bruckert E, Catapano AL, Kuivenhoven JA, Pajukanta P, Ray K, Stalenhoef AF, Stroes E, Taskinen MR, Tybjærg-Hansen A; European Atherosclerosis Society Consensus Panel. Familial hypercholesterolaemia is underdiagnosed and undertreated in the general population: guidance for clinicians to prevent coronary heart disease: consensus statement of the European Atherosclerosis Society. Eur Heart J 2013; 34: 3478-3490.
17) Malyutin AG, Musalgaonkar S, Patchett S, Frank J, Johnson AW. Nmd3 is a structural mimic of eIF5A, and activates the cpGTPase Lsg1 during 60S ribosome biogenesis. EMBO J 2017; 36: 854-868.
18) Pantazi A, Quintanilla A, Hari P, Tarrats N, Parasyraki E, Dix FL, Patel J, Chandra T, Acosta JC, Finch AJ. Inhibition of the 60S ribosome biogenesis GTPase LSG1 causes endoplasmic reticular disruption and cellular senescence. Aging Cell 2019; 18: e12981.
19) Nagane M, Yasui H, Kuppusamy P, Yamashita T, Inanami O. DNA damage response in vascular endothelial senescence: Implication for radiation-induced cardiovascular diseases. J Radiat Res 2021; 62: 564-573.
20) Liu J, Li H, Mao A, Lu J, Liu W, Qie J, Pan G. DCAF13 promotes triple-negative breast cancer metastasis by mediating DTX3 mRNA degradation. Cell Cycle 2020; 19: 3622-3631.
21) Zhou ZX, Ren Z, Yan BJ, Qu SL, Tang ZH, Wei DH, Liu LS, Fu MG, Jiang ZS. The role of ubiquitin E3 ligase in atherosclerosis. Curr Med Chem 2021; 28: 152-168.
22) Qian LL, Liu XY, Yu ZM, Wang RX. BK channel dysfunction in diabetic coronary artery: Role of the E3 ubiquitin ligases. Front Physiol 2020; 11: 453.
23) Gao ZHJ, Zhu TT, Niu XR, Liu EW, Fu ZHF. Review on research progress of chemical constituents, pharmacological activities of Spatholobi Caulis. Journal of Liaoning University of Traditional Chinese Medicine 2021; 23: 1-18.
24) Monemi S, Spaeth G, DaSilva A, Popinchalk S, Ilitchev E, Liebmann J, Ritch R, Héon E, Crick RP, Child A, Sarfarazi M. Identification of a novel adult-onset primary open-angle glaucoma (POAG) gene on 5q22.1. Hum Mol Genet 2005; 14: 725-733.

25) Gallenberger M, Meinel DM, Kroeber M, Wegner M, Milkereit P, Bösl MR, Tamm ER. Lack of WDR36 leads to preimplantation embryonic lethality in mice and delays the formation of small subunit ribosomal RNA in human cells in vitro. Hum Mol Genet 2011; 20: 422-435.

26) Bernstein KA, Gallagher JE, Mitchell BM, Granneman S, Baserga SJ. The small-subunit processome is a ribosome assembly intermediate. Eukaryot Cell 2004; 3: 1619-1626.

27) Skarie JM, Link BA. The primary open-angle glaucoma gene WDR36 functions in ribosomal RNA processing and interacts with the p53 stress-response pathway. Hum Mol Genet 2008, 17: 2474-2485.

28) Zeng M, Zhu L, Li L, Kang C. miR-378 suppresses the proliferation, migration and invasion of colon cancer cells by inhibiting SDAD1. Cell Mol Biol Lett 2017; 22: 12.

29) Jing L, Li S, Wang J, Zhang G. Long non-coding RNA small nucleolar RNA host gene 7 facilitates cardiac hypertrophy via stabilization of SDA1 domain containing 1 mRNA. J Cell Biochem 2019; 120: 15089-15097

30) Li H, Gao F, Wang X, Wu J, Lu K, Liu M, Li R, Ding L, Wang R. Circulating microRNA- 378 levels serve as a novel biomarker for assessing the severity of coronary stenosis in patients with coronary artery disease. Biosci Rep 2019; 5: BSR20182016

31) Gromadka R, Rytka J. The KRR1 gene encodes a protein required for 18S rRNA synthesis and 40S ribosomal subunit assembly in Saccharomyces cerevisiae. Acta Biochimica Polonica 2000; 47: 993-1005.

32) Bi LR, Wang B, Luo N, Hou XW, Chen QY, Lian R, Zhao y, Song Cl. Biological function of cyclic RNA and its research progress in coronary atherosclerotic heart disease. Chinese Circulation Journal 2018; 33: 1141-1144.

33) Takagi M, Sueishi M, Saiwaki T, Kametaka A, Yoneda Y. A novel nucleolar protein, NIFK, interacts with the forkhead associated domain of Ki-67 antigen in mitosis. J Biol Chem 2001; 276: 25386-25391.

34) Pan WA, Tsai HY, Wang SC, Hsiao M, Wu PY, Tsai MD. The RNA recognition motif of NIFK is required for rRNA maturation during cell cycle progression. RNA Biol 2015; 12: 255-267.

35) Men H, Cai H, Cheng Q, Zhou W, Wang X, Huang S, Zheng Y, Cai L. The regulatory roles of p53 in cardiovascular health and disease. Cell Mol Life Sci 2021; 78: 2001-2018.